Atmospheric Environment 43 (2009) 1932–1939

Contents lists available at ScienceDirect

Atmospheric Environment

journal homepage: www.elsevier.com/locate/atmosenv

Aerosol physical, chemical and optical properties during the Rocky Mountain Airborne Nitrogen and Sulfur study

E.J.T. Levin [a,*], S.M. Kreidenweis [a], G.R. McMeeking [a], C.M. Carrico [a], J.L. Collett, Jr. [a], W.C. Malm [b]

[a] Department of Atmospheric Science, Colorado State University, 1371 Campus Delivery, Fort Collins, CO 80523-1371, USA
[b] National Park Service/Cooperative Institute for Research in the Atmosphere, Colorado State University, Fort Collins, CO 80523-1375, USA

ARTICLE INFO

Article history:
Received 4 September 2008
Received in revised form
18 December 2008
Accepted 18 December 2008

Keywords:
Visibility
Remote aerosol concentrations
Remote aerosol composition
Rocky Mountain National Park air quality

ABSTRACT

During the Rocky Mountain Airborne Nitrogen and Sulfur (RoMANS) study, conducted during the spring and summer of 2006, a suite of instruments located near the eastern boundary of Rocky Mountain National Park (RMNP) measured aerosol physical, chemical and optical properties. Three instruments, a differential mobility particle sizer (DMPS), an optical particle counter (OPC), and an aerodynamic particle sizer (APS), measured aerosol size distributions. Aerosols were sampled by an Interagency Monitoring of Protected Visual Environments (IMPROVE) sampler and a URG denuder/filter-pack system for compositional analysis. An Optec integrating nephelometer measured aerosol light scattering. The spring time period had lower aerosol concentrations, with an average volume concentration of $2.2 \pm 2.6\ \mu m^3\ cm^{-3}$ compared to $6.5 \pm 3.9\ \mu m^3\ cm^{-3}$ in the summer. During the spring, soil was the single largest constituent of $PM_{2.5}$ mass, accounting for 32%. During the summer, organic carbon accounted for 60% of the $PM_{2.5}$ mass. Sulfates and nitrates had higher fractional contributions in the spring than the summer. Variability in aerosol number and volume concentrations and in composition was greater in the spring than in the summer, reflecting differing meteorological conditions. Aerosol scattering coefficients (b_{sp}) measured by the nephelometer compared well with those calculated from Mie theory using size distributions, composition data and modeled RH dependent water contents.

1. Introduction

The Rocky Mountain Airborne Nitrogen and Sulfur (RoMANS) study was conducted at various sites throughout Colorado and surrounding states in two phases during the spring and summer of 2006. This work focuses on aerosol data collected at the RoMANS core site, located near the eastern boundary of Rocky Mountain National Park (RMNP) 8 km south of Estes Park, Co. at an elevation of 2750 m. The spring study period lasted from 23 March through 30 April and the summer period from 6 July though 12 August. The overarching goals of RoMANS included characterizing wet and dry deposition fluxes of sulfur and nitrogen in RMNP as well as identifying source types and regions for these species. Since dry deposition of particulate matter and wet deposition of precipitation scavenged particulate matter are contributors to N and S deposition fluxes, characterization of aerosol concentrations and composition is an important component of understanding pollutant deposition fluxes in the region.

The particles that contribute to N and S deposition also affect visibility. Since 1988 the Interagency Monitoring of Protected Visual Environments (IMPROVE) program has measured light scattering aerosols in federally protected areas, such as RMNP (Malm et al., 2004). In 1999 the Environmental Protection Agency enacted the Regional Haze Rule which requires all federal Class I areas (national parks and wilderness areas) to return visibility to natural conditions within 60 years (Malm and Hand, 2007). In order to reach this objective, it is imperative to know the species, and sources of these species, that contribute to visibility degradation. The goal of this paper is to examine aerosol concentration and speciation in RMNP during the two RoMANS study periods and the effects these aerosols have on visibility in the park.

2. Methods

Three instruments located at the RoMANS core site measured aerosol number size distributions with 15-min time resolution: a differential mobility particle sizer (DMPS; TSI 3085), an optical particle counter (OPC; PMS LASAIR 1003) and an aerodynamic particle sizer (APS; TSI 3021). These three instruments measured over the ranges 0.04–0.63 μm, 0.39–0.95 μm and 1.0–20 μm

* Corresponding author.
E-mail address: elevin@atmos.colostate.edu (E.J.T. Levin).

1352-2310/$ – see front matter © 2008 Elsevier Ltd. All rights reserved.
doi:10.1016/j.atmosenv.2008.12.042

respectively. Calibrations were checked twice during the spring study period and three times during the summer period with polystyrene latex (PSL) spheres of known sizes.

The sizing instruments were housed inside a temperature-controlled mobile lab. Sample flow at 0.6 LPM was pulled through an inlet in the roof and then passed through a Perma Pure dryer (Perma Pure Inc., Toms River, NJ) which dried the sample to RH < 10% by supplying dry air to the sheath of the dryer. After the dryer, the flow was split isokinetically into two 0.3 LPM flows which were sent to the OPC and DMPS. Because the OPC operated at a flow rate of only 0.028 LPM, the excess 0.272 LPM was siphoned off before the OPC inlet using a critical orifice to control the flow. To avoid losses of larger particles, the APS sampled through a separate inlet, with no bends, at 5.0 LPM. The APS sample was dried using a heating tape wrapped around the inlet tube which heated the flow to ~35 °C, thus reducing RH < 15%. The sample flow was exposed to this heated region for about 0.5 s. This short residence time limits the loss of volatile particles (An et al., 2007) yet is still long enough for any water on the aerosol to react to the lower RH (Snider and Petters, 2008). The inlets for both the DMPS/OPC and APS were approximately 5 m above ground level.

A URG denuder and filter pack system collected 24-h samples to determine concentrations of SO_4^{2-}, NO_3^-, Cl^-, Na^+, K^+, Ca^{2+}, Mg^{2+} and NH_4^+ ions. The URG system, described in detail by Lee et al. (2004), consists of a 2.5 μm aerodynamic size cut cyclone followed in series by two annular denuders, a filter pack and then a third denuder. The first denuder in the series was coated with Na_2CO_3 and the second with H_3PO_3 to collect gas phase nitric acid and ammonia, respectively. The nylon filter (Pall Corp. Nylasorb, 1.0 μm pore size) collected particulate matter and the third denuder captured any volatilized NH_4^+. The nylon filter has been shown to retain any volatilized nitric acid (Yu et al., 2005). Samples were run from 8:00 AM to 8:00 AM MST. Flow was controlled by a mass flow controller and verified by an in-line dry gas meter. Aqueous extracts of filters and denuders were analyzed by IC at Colorado State University using methods similar to those outlined by Yu et al. (2005). The URG sampling height was approximately 3 m above ground level.

The RoMANS main site was located at the RMNP IMPROVE sampling site, which has been in place since 1988. The IMPROVE sampler, described by DeBell et al. (2006), consists of four modules, each with its own pump, size cutting cyclone and sample substrate. Three modules have a 2.5 μm aerodynamic size cut ($PM_{2.5}$) and collect aerosols onto Teflon, nylon and quartz filter substrates. The fourth module uses a 10 μm aerodynamic size cut (PM_{10}) and collects particles onto a Teflon filter. The two Teflon filters are weighed before and after sampling in a clean, climate controlled room kept at an RH of 20–40%, to determine total gravimetric mass loading. The $PM_{2.5}$ Teflon filter is also analyzed by X-ray fluorescence analysis for the common soil elements Al, Si, Ca, K, Fe, Ti, Mg and Na. Concentrations of NO_3^- and SO_4^{2-} are determined by IC analysis of an aqueous extract of the nylon filter and the quartz filter is analyzed via thermal optical reflectance (TOR) for organic and elemental carbon. The analysis techniques are described in greater detail by DeBell et al. (2006). During RoMANS, the IMPROVE sampler was run on the same schedule as the URG sampler, daily from 8:00 AM to 8:00 AM MST, which is different from the routine network sampling schedule.

An Optec NGN-2 integrating nephelometer located at the IMPROVE site measured ambient aerosol scattering. This instrument has an open-air inlet, which does not deliberately exclude any particles by size. The nephelometer uses a Lambertian light source with an effective wavelength of 550 nm and detects scattered light over the range 5°–175° (Optec NGN-2 Instrument Manual). An internal sensor measures the RH of the sample in the inlet. The instrument was automatically calibrated with HEPA filtered air every six hours and HFC-134A (SUVA) once a day.

2.1. Data analysis

Particle losses in the sizing instrument sampling lines and Perma Pure dryer were calculated based on the procedure in Hand (2001). Particle loss was generally below 10%, except for particles in the largest OPC size bin, for which losses increased to 45%. Aerosol concentrations were adjusted to account for these losses. Losses in the APS inlet were assumed to be negligible due to its size and vertical geometry. Data from both the sizing system and the Optec nephelometer were screened to remove spikes in the data, defined as a greater than 100% difference between two adjacent data points. The Optec data were also filtered to remove times when RH > 90%.

Because the three sizing instruments all measure over different diameter ranges and exploit different aerosol characteristics, the output from the instruments has to be reconciled to produce one continuous size distribution. This was done following the alignment method developed by Hand and Kreidenweis (2002). This technique was previously successfully employed during the Big Bend Regional Aerosol and Visibility Observational (BRAVO) study in 1999 (Hand et al., 2002) and the Yosemite Aerosol Characterization Study (YACS) in 2002 (McMeeking et al., 2005). Data from the three instruments are first fit to a common diameter grid using a Twomey fit (Winklmayr et al., 1990). The alignment method then reconciles DMPS, OPC and APS data in two separate steps.

The first step fits the OPC data to the DMPS by adjusting the real refractive index (n), used to define the particle size corresponding to the OPC bins, since the OPC output is a function of this parameter. OPC response to different n values was characterized by using size selected aerosols of known n. By performing this test with oleic acid, $n = 1.46$, ammonium sulfate, $n = 1.53$, and using the manufacture's PSL calibrations, $n = 1.588$, OPC response curves can be calculated for each bin (Hand and Kreidenweis, 2002). Table 1 gives the lower bin limits for each OPC channel as a function of n.

The alignment process scans through n, from 1.400 to 1.600 in increments of 0.005, and adjusts the OPC output based on the previously calculated OPC response curves. The DMPS data are also inverted in this step of the alignment. The DMA is run without an impactor which would give a known upper size limit to sampled particles. Instead, OPC data are assumed to represent singly charged particles and are used to correct for multiply charged particles in the DMA inversion (Hand and Kreidenweis, 2002). The fit between the refractive index adjusted OPC and inverted DMPS data is tested using the χ^2 statistic and the refractive index leading to the lowest χ^2 is selected as the best-fit.

The APS measures aerodynamic diameter (D_a) which is related to equivalent spherical diameter (D_e) via the equation (Hinds, 1999)

$$D_e = D_a\left(\frac{\rho_0}{\rho_e}\right)^{\frac{1}{2}} \quad (1)$$

Table 1
OPC lower bin limits as determined by calibration aerosols with different real refractive indices.

Channel	PSL, $m = 1.588$ [μm]	$(NH_4)_2SO_4$, $m = 1.53$ [μm]	Oleic acid, $m = 1.46$ [μm]
1	0.1	0.130	0.150
2	0.2	0.241	0.261
3	0.3	0.363	0.369
4	0.4	0.548	0.585
5	0.5	0.730	0.770
6	0.7	0.810	0.890

where ρ_0 is 1.0 g cm^{-3}. The second step of the alignment fits the APS data to the aligned OPC data by scanning through density from 1.20 to 3.00 g cm^{-3} in 0.05 g cm^{-3} increments. The APS output is converted to equivalent spherical diameter using the assumed effective density (ρ_e), which includes shape factor, and compared to the aligned OPC data in the overlap region using χ^2, with the best-fit density taken as that where χ^2 is a minimum.

The final output from the alignment is a dry aerosol number distribution between 0.04 and 20 μm expressed as $dN/d\log_{10}D_p$ evaluated at 96 diameters with a base 10 logarithmic bin width of 0.03. The alignment program also records the real refractive index and density resulting in the best-fit at each measurement point. Hand et al. (2002), using the same technique, estimated uncertainties of up to 10% in volume concentrations, 2% in accumulation mode geometric mean diameter (D_{gv}) and 20% in coarse mode D_{gv}.

3. Aerosol size distributions

Volume distributions ($dV/d\log_{10}D_p$) were calculated from the number distributions and both number and volume distribution statistics were calculated using the equations in Seinfeld and Pandis (2006). We also calculated integrated total number and volume concentrations. Table 2 lists the mean and one standard deviation for total aerosol number and volume concentrations as well as accumulation and coarse mode concentrations and mode statistics.

While measured aerosol number concentrations were generally low in RMNP, they were significantly higher during the summer than the spring. The mean, and one standard deviation, aerosol number concentration in the spring was 880 ± 770 cm^{-3} while in the summer it was 2080 ± 940 cm^{-3} and total integrated volume concentrations were 2.2 ± 2.6 μm^3 cm^{-3} in the spring and 6.5 ± 3.9 μm^3 cm^{-3} in the summer. Although these standard deviations are large, aerosol concentrations (both number and volume) were significantly different between spring and summer at the 95% confidence level using a two tailed *t*-test.

Aerosol distributions were split into accumulation and coarse modes based on the minimum values between the modes in the volume distributions. This minimum occurred at an average value of 0.63 μm in the spring and 0.74 μm in the summer. In the spring, the coarse mode dominated the volume distribution, accounting for 60% of the total aerosol volume. In the summer, however, the accumulation mode made up 60% of the aerosol volume.

Geometric mean diameters (D_g) and standard deviations (σ_g) were calculated for each number (subscript n) and volume (subscript v) distribution. The accumulation mode D_{gv} remained constant throughout both study periods with an average value of 0.2 ± 0.03 μm. For the coarse mode, however, D_{gv} increased significantly in the summer when its average value was 4.7 ± 0.9 μm compared to 3.4 ± 1.3 μm in the spring. We note that, if the particle number distributions were cut off at 10 μm, as would occur in a PM_{10} sampler, the computed mean D_{gv} for the coarse mode decreased: spring, 2.6 μm, and summer, 3.2 μm, indicating that the PM_{10} sampler missed some fraction of the coarse mode aerosol. In the spring, the average σ_{gv} for the accumulation and coarse modes were 1.8 ± 0.1 μm and 2.0 ± 0.2 μm, respectively. In the summer, both modes of the volume distribution were narrower with σ_{gv} of 1.6 ± 0.07 for the accumulation mode and 1.9 ± 0.1 for the coarse mode.

In addition to having lower aerosol concentrations, the spring also exhibited greater variability. The number concentration varied 88% about its mean during the spring and only 42% during the summer. Percent variations about the mean for the volume concentration, coarse mode D_{gv}, and σ_{gv} for both modes were also larger in the spring than in the summer.

4. Aerosol composition

Data from the IMPROVE and URG samplers were used to determine $PM_{2.5}$ aerosol composition. Ammonium, sulfate and nitrate concentrations were taken from the URG data while IMPROVE data were used for all other species. Malm et al. (submitted for publication) discuss the comparisons between duplicate measurements from the two samplers. While SO_4^{2-} concentrations were in generally good agreement, NO_3^- concentrations differed by 15–20%, and the IMPROVE NH_4^+ concentrations were roughly 50% less than those from the URG sampler. The discrepancies are likely due to the lack of front-end and backup denuders on the IMPROVE sampler, and thus the URG data are considered to be more reliable. A charge balance was performed with the URG data (Fig. 1). The ratio of cations to anions was 0.9 ± 0.2 in the spring and 1.2 ± 0.2 in the summer. The slightly high value in the summer indicates an excess of measured ammonium, which could be accounted for by oxalate. We did not analyze samples for oxalate; however, its mass is expected to be accounted for in the bulk organic carbon measurement, so we do not separately compute it. Since it is a minor component, it has no discernable effect on any of our following calculations.

Following standard IMPROVE procedures (Pitchford et al., 2007), we assumed that reconstructed fine mass (RCFM) was completely accounted for by the following components:

$$[\mathrm{RCFM}] = [\mathrm{OMC}] + [\mathrm{SOIL}] + [\mathrm{SULFATE}] + [\mathrm{NITRATE}] + [\mathrm{LAC}] \quad (2)$$

where the terms are the mass concentrations of organics, soil, sulfates, nitrates and light absorbing carbon respectively. We have neglected the contribution of sea salt, which was insignificant. Each of these components is computed as follows.

Total organic mass concentrations [OMC] were computed by multiplying the mass concentration of organic carbon [OC] by a coefficient to account for the mass of other elements, such as H, O and N, in the organic molecule. The standard IMPROVE algorithm uses an [OC] coefficient of 1.8 for every site (Pitchford et al., 2007). There can be great variability in organic molecules, however, and Malm and Hand (2007) found that an [OC] multiplier of 1.7 worked best for the RMNP IMPROVE site. We also found that a value of 1.7 gave the best agreement for the spring data, and thus applied the following:

$$[\mathrm{OMC}]_{\mathrm{spring}} = 1.7[\mathrm{OC}] \quad (3)$$

Table 2
Mean and standard deviations for number and volume aerosol concentrations and mode statistics. Concentration units are: number [cm^{-3}], volume [μm^3 cm^{-3}].

		Total conc.	Accumulation			Coarse		
			Conc.	D_g [μm]	σ_g	Conc.	D_g [μm]	σ_g
Spring	Number	880 ± 770	880 ± 770	0.08 ± 0.01	1.7 ± 0.10	0.64 ± 0.55	1.1 ± 0.08	1.5 ± 0.11
	Volume	2.2 ± 2.6	0.9 ± 0.8	0.20 ± 0.03	1.8 ± 0.12	1.6 ± 1.6	3.4 ± 1.3	2.0 ± 0.19
Summer	Number	2080 ± 940	2070 ± 930	0.09 ± 0.02	1.8 ± 0.08	0.46 ± 0.34	1.2 ± 0.11	1.6 ± 0.08
	Volume	6.5 ± 3.9	3.7 ± 2.1	0.21 ± 0.03	1.6 ± 0.07	2.8 ± 2.4	4.7 ± 0.89	1.9 ± 0.11

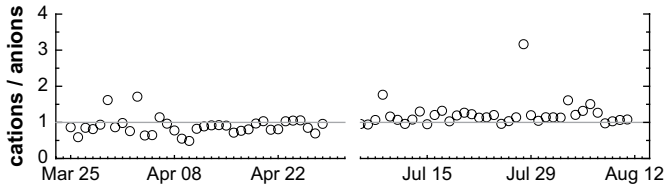

Fig. 1. Ratio of cations to anions from the URG data in equivalent units. Grey line indicates charge balance.

In the summer, using a coefficient of 1.7 underestimated the gravimetric mass. To achieve closure between gravimetric and reconstructed fine mass in summer, [OC] was multiplied by 1.95.

$$[\mathrm{OMC}]_{\mathrm{summer}} = 1.95[\mathrm{OC}] \quad (4)$$

Soil mass concentrations were computed using:

$$[\mathrm{SOIL}] = 2.2[\mathrm{Al}] + 2.49[\mathrm{Si}] + 1.63[\mathrm{Ca}] + 2.42[\mathrm{Fe}] + 1.94[\mathrm{Ti}] \quad (5)$$

where the terms are mass concentrations of aluminum, silicon, calcium, iron and titanium and the coefficients account for the common oxides of these soil elements (Malm et al., 2004). These coefficients are all consistent with standard IMPROVE assumptions.

In contrast to the standard IMPROVE assumption, we did not compute total sulfate compound mass assuming the sulfate ion was fully ammoniated. Sulfate ammoniation was allowed to vary among NH_4HSO_4, $(NH_4)_3H(SO_4)_2$ and $(NH_4)_2SO_4$ depending on the measured ratio of moles of ammonium to moles of sulfate (Fig. 2). In the spring, the mole ratio varied between 1 and 5 so it was assumed that the various forms of ammoniated sulfate were present in the appropriate proportions for each day. In summer, the molar ratio was always greater than or equal to two, so only $(NH_4)_2SO_4$ was assumed to be present.

Light absorbing carbon mass concentration [LAC] was equated to that of elemental carbon determined from the TOR analysis.

To test the assumption that RCFM completely accounts for $PM_{2.5}$ mass, as well as the assumptions in calculating the RCFM components, RCFM was plotted against the measured $PM_{2.5}$ gravimetric mass (GM). These data showed very good agreement using the above assumptions with an R^2 value of 0.96 in the spring and 0.98 in the summer and a regression line slope of 1.0 for both seasons.

Averaged over each study period, soil was the single largest constituent of $PM_{2.5}$ in the spring, while organic carbon dominated $PM_{2.5}$ in the summer. Also, both sulfate and nitrate contributed significantly more to aerosol mass in the spring than the summer. Similar to what was seen above with aerosol size distributions, spring composition also had greater variability with large spikes in soil concentration on the 9th, 16th and 22nd of April (Fig. 3). These spikes in soil may be the result of long range Asian dust transport which often affects the western US in the spring (Malm et al., 2004), although the transport patterns associated with Asian dust also

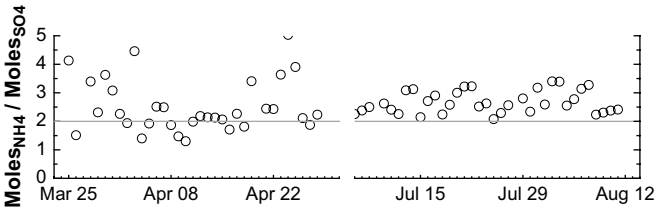

Fig. 2. Ratio of moles of ammonium to moles of sulfate. Times with points above the grey line are assumed to have fully ammoniated sulfate.

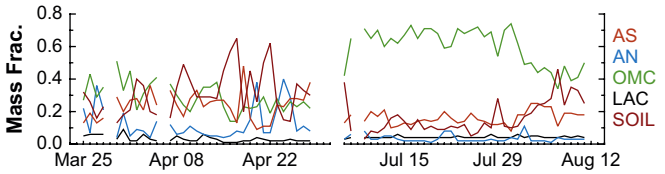

Fig. 3. Mass fraction of $PM_{2.5}$ components: ammoniated sulfate (red), ammonium nitrate (blue) organic carbon (green), elemental carbon (black) and soil (brown). (For interpretation of the references to color in this figure legend, the reader is referred to the web version of this article.)

frequently move through the southwestern U.S. and can pick up dusts from these regions (Richardson et al., 2007). In the summer, aerosol composition remained more constant, with organics accounting for over half of $PM_{2.5}$ throughout most of the study period. Biomass burning can be a significant source of organic species and often affects aerosol composition and loading throughout the western US during the summer months (Park et al., 2007).

Table 3 shows the average, and one standard deviation, mass fractions of each RCFM component during the two time periods. The same table also shows the average mass fractions from the IMPROVE data for the months of April and July averaged over 1991–2006. In calculating the historical aerosol composition, we used the same [OC] coefficients as used for the RoMANS data, but since NH_4^+ is not measured in the network, the historical data assume ammonium sulfate. Aerosol composition during the RoMANS spring period was very similar to the historical data with no component showing a significant difference from the historical average. As with the RoMANS summer data, OMC dominated aerosol composition in the historical data, although its mass fraction was slightly lower than that measured during RoMANS. Also, during the summer, the fraction attributed to ammoniated sulfate was lower than that in the historical record. Average, and standard deviation, daily $PM_{2.5}$ mass loading during the two RoMANS periods were 3.1 ± 1.4 and $5.6 \pm 2.2\ \mu g\ m^{-3}$. Historical values for these two time periods are 3.4 ± 1.7 and $5.3 \pm 2.5\ \mu g\ m^{-3}$.

We calculated dry aerosol refractive index (m_{comp}) and density (ρ_{comp}) from the daily composition data, assuming internal mixing, using (Hasan and Dzubay, 1983):

$$\rho_{comp}^{-1} = \sum_i \frac{X_i}{\rho_i} \quad (6)$$

$$m_{comp} = \rho_{comp} \sum_i \frac{X_i n_{i,i}}{\rho_i} - \rho_{comp} \sum_i \frac{X_i k_i i}{\rho_i} \quad (7)$$

where X_i, ρ_i, n_i and k_i are respectively the mass fraction, density, real refractive index and imaginary refractive index for species i. Table 4 gives values for the individual species densities and refractive indices used here.

Table 3
Mean and one standard deviation $PM_{2.5}$ mass fractions for aerosol components during the two RoMANS periods as well as historical means and standard deviations for April and July from 1991 to 2006.

		AS	AN	OMC	LAC	SOIL
Spring	RoMANS	0.24 ± 0.08	0.13 ± 0.1	0.29 ± 0.09	0.03 ± 0.02	0.32 ± 0.14
	Historical	0.31 ± 0.06	0.15 ± 0.05	0.26 ± 0.06	0.03 ± 0.01	0.24 ± 0.09
Summer	RoMANS	0.16 ± 0.04	0.03 ± 0.02	0.60 ± 0.12	0.04 ± 0.01	0.16 ± 0.10
	Historical	0.24 ± 0.05	0.05 ± 0.02	0.51 ± 0.06	0.04 ± 0.01	0.16 ± 0.04

Table 4
Densities and refractive indices for species used in reconstructed fine mass calculations.

Species	Density [g cm^{-3}]	Refractive index
NH_4HSO_4	1.78[a]	1.48[a]
$(NH_4)_3H(SO_4)_2$	1.83[a]	1.53[a]
$(NH_4)_2SO_4$	1.76[a]	1.53[a]
NH_4NO_3	1.73[b]	1.55[b]
Organic carbon	1.40[c]	1.55[c]
Elemental carbon	2.00[a]	1.96 – 0.66i[a]
SiO_2	2.32[d]	1.49[d]
Al_2O_3	3.97[d]	1.77[d]
Fe_2O_3	5.24[d]	3.01[d]
CaO	3.30[d]	1.83[d]
TiO_2	4.23[d]	2.58[d]
H_2O	1.00[d]	1.33[d]

[a] Stelson (1990).
[b] Tang (1996).
[c] Dick (2000).
[d] Lide (2008).

Fig. 4 shows the real (n_{comp}) and imaginary (k_{comp}) dry refractive indices calculated from composition for both study periods plotted in red and blue respectively. The black line is the best-fit refractive index retrieved for the dry aerosol by the alignment method ($m_{retrieved}$). The average refractive index calculated from composition data was $n_{comp} = 1.59 \pm 0.016$, $k_{comp} = 0.020 \pm 0.012$ for the spring and $n_{comp} = 1.57 \pm 0.009$, $k_{comp} = 0.023 \pm 0.004$ for the summer. The average retrieved refractive indices were in good agreement with these estimates, with $m_{retrieved} = 1.58 \pm 0.011$ and $m_{retrieved} = 1.56 \pm 0.011$ for the two study periods.

5. Data intercomparison

5.1. Mass/volume comparison

Aerosol density was estimated from IMPROVE $PM_{2.5}$ gravimetric mass concentrations and aligned $PM_{2.5}$ volume concentrations. The slope of the zero-intercept regression line through these points gives an estimate of the aerosol density for each time period: $\rho = 1.96 \pm 0.19$ g cm^{-3} for the spring and $\rho = 1.40 \pm 0.06$ g cm^{-3} for the summer. The spring density agrees with that calculated from composition, $\rho_{comp} = 1.9 \pm 0.15$ g cm^{-3}, within the uncertainty. However, the summer aerosol density estimated by the above method is significantly less than that calculated from composition, $\rho_{comp} = 1.62 \pm 0.11$ g cm^{-3}. Agreement within the uncertainty can be achieved, however, if the density of organics (ρ_{oc}) in summertime is assumed to be 1.2 g cm^{-3} instead of 1.4 g cm^{-3} as listed in Table 4. This results in an average composition derived density of $\rho_{comp} = 1.46 \pm 0.11$ g cm^{-3}. We note that measurement and model assumption uncertainties and biases also contribute to the observed slope between volume and mass concentrations, and the adjustment of the average densities is only one way to explain this slope. However, the requirement for a different OC-to-OMC conversion factor to achieve mass closure in summertime suggests it is not unreasonable to expect other organic aerosol properties to also differ between these seasons. Both of these assumed ρ_{oc} values are within the ranges cited by Turpin and Lim (2001), and induce only minor changes (2% or less) in the computed optical properties. The R^2 value for the mass/volume comparison is much larger in the summer, 0.96 than the spring, 0.66, indicating aerosol density varied more in the spring than in the summer, consistent with the more variable composition in the spring.

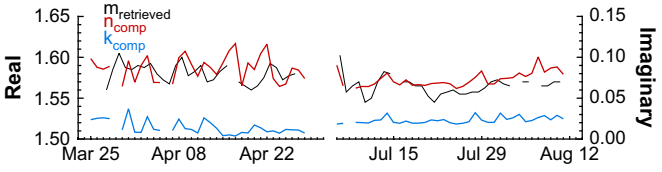

Fig. 4. Daily averaged effective refractive index retrieved from alignment method (black) and real (red) and imaginary (blue) refractive indices calculated from aerosol composition. (For interpretation of the references to color in this figure legend, the reader is referred to the web version of this article.)

5.2. Scattering comparison

Aerosol scattering coefficients can be calculated using Mie theory if aerosol size distribution and refractive index are known and if spherical particles are assumed. We used m_{comp} values to calculate dry light scattering efficiencies (Q_{scat}) for each alignment bin midpoint diameter. We assumed that the aerosol in the fine mode was internally mixed, and that the fine mode aerosol composition was that of the measured $PM_{2.5}$ fraction. The coarse mode was assumed to contain only soil. Because composition data have only daily temporal resolution, we assumed that these values apply from 8:00 AM to 8:00 AM each day. Using the calculated Q_{scat} values, we then calculated dry aerosol scattering coefficients (b_{sp}) in Mm^{-1} using the following equation (Seinfeld and Pandis, 2006)

$$b_{sp} = \sum_i \frac{\pi D_{p,i}^2}{4} N_i Q_{scat,i} \quad (8)$$

where $D_{p,i}$ is the bin midpoint diameter [μm], N_i is particle number concentration [cm^{-3}], and the sum is over all bins. The calculation was done for a wavelength of 550 nm, and for each 15-min size distribution sampling period, initially neglecting any changes in the measured dry aerosol size distributions due to water uptake. The calculated b_{sp} values, as well as ambient b_{sp} measured by the nephelometer, were averaged to an hourly time interval for comparisons. The nephelometer data were not adjusted to account for any measurement nonidealities.

In the spring, the calculated dry b_{sp} underestimated measured b_{sp}, especially for the higher values. There was much better agreement during the summer. The slope of the regression line through the calculated versus measured data points, using simple linear regression, is 0.84 in the summer compared with 0.4 in the spring (Table 5). The summer data are also more highly correlated, with an $R^2 = 0.82$ while for the spring $R^2 = 0.59$.

Much of the discrepancy between the measured and calculated b_{sp} values in the spring can be accounted for by the effects of humidity. Aerosol water uptake affects both particle size and refractive index and can have a large effect on b_{sp} (Malm and Day,

Table 5
Average and standard deviation values for b_{sp} measured by the Optec and b_{sp} calculated using dry aerosols (Mie_{dry}), wet accumulation mode aerosols (Mie_{wet_acc}) and wet accumulation plus coarse mode aerosols (Mie_{wet_total}) [Mm^{-1}]. Regression statistics, from simple linear regression, show the agreement between calculated and measured values for each case.

		Ave.	Std. Dev.	R^2	Slope	Intercept
Spring	Optec	6.1	9.1			
	Mie_{dry}	4.2	4.9	0.59	0.40	2.07
	Mie_{wet_acc}	5.3	6.5	0.90	0.63	1.70
	Mie_{wet_total}	5.5	6.5	0.87	0.66	2.06
Summer	Optec	14.5	15.7			
	Mie_{dry}	14.8	14.9	0.82	0.84	3.46
	Mie_{wet_acc}	15.0	14.9	0.87	0.89	3.24
	Mie_{wet_total}	15.8	15.8	0.90	0.96	2.26

2001). To account for water uptake we used the online Aerosol Inorganics Model (AIM) (Wexler and Clegg, 2002) to generate water uptake curves as a function of relative humidity for each of the assumed nitrate and sulfate species. The AIM code was run in metastable mode at 298.15 K. Relative humidity was scanned from 0.1 to 0.99 and polynomial fits constructed. We used these curves to calculate the volume of water associated with each species at every time point for the ambient RH measured by the Optec nephelometer, assuming that water activity is equivalent to RH, and then calculated total water associated with the aerosol using the ZSR assumption (Stokes and Robinson, 1966). We assumed that soil and carbonaceous species had zero water uptake (Carrico et al., 2005). This new composition was then used to calculate the aerosol sizes and refractive indices used by the Mie code to reconstruct scattering.

As can be seen in Table 5, including aerosol water uptake in the calculated b_{sp} (Mie_{wet_total}) improves the agreement with measured b_{sp} for both seasons. In the spring, the slope of the regression line increased to 0.66 and in the summer to 0.96. Also, the R^2 values for both seasons increased, 0.87 in the spring and 0.90 in the summer, when water uptake was accounted for. We note that our calculations show that our choices for model inputs produced estimates of scattering coefficients that were consistent with the measurements, but that alternative assumptions – e.g., regarding the mixing of constituents within individual particles, the water uptake properties of organic carbon, and other assumptions – could also be applied.

Based on our calculations, aerosol water uptake played a much greater role in b_{sp} during the spring than the summer. During the spring, calculated b_{sp} increased by 20% on average when water was included. For the highest b_{sp} values, calculated scattering almost doubled. These high scattering points (indicated in grey in Fig. 5a) are all from April 24 to 25 when RH was high, greater than 80%, and nitrate and sulfate species accounted for roughly 40% and 25%, respectively, of $PM_{2.5}$ mass concentrations (See Fig. 3). These species have large water concentrations associated with them for RH > 80% and therefore lead to much higher b_{sp} values. However, even with the drastic increase in calculated b_{sp} these values are still lower than the measured b_{sp} values, leading to the regression line slope less than 1. Because these points all fall during the time period with the highest RH, this could indicate a slight bias in the RH measurements, as small errors lead to larger discrepancies at higher RH values. The underprediction of b_{sp} during this time period could also indicate that our assumed composition and/or assumed mixing state are incorrect during this time. We note that the data show no evidence of the presence of highly hygroscopic sea salt particles, and the coarse mode volume fraction was low, about 10%, so errors in the assumptions regarding the contributions to b_{sp} from those factors are probably not important in explaining the discrepancies. If these points are removed, calculated and measured b_{sp} show very good agreement when water uptake is included (red line in Fig. 5a).

In the summer, the differences between wet and dry scattering coefficients are much smaller, with an average increase of only 6%. The differences between the two seasons are due to aerosol composition and not differences in humidity. The average humidity was actually higher in the summer, 51% versus 41%, and the humidity was greater than 60% more often in the summer, 27% of the time, than in the spring, 17% of the time. This difference in aerosol hygroscopicity between the spring and summer is consistent with seasonal aerosol composition. In the summer the mean 24-h composition was dominated by carbonaceous material with little or no hygroscopic growth.

In Table 5 Mie_{wet_acc} refers to b_{sp} calculated using only humidified accumulation mode aerosols. By comparing these values to

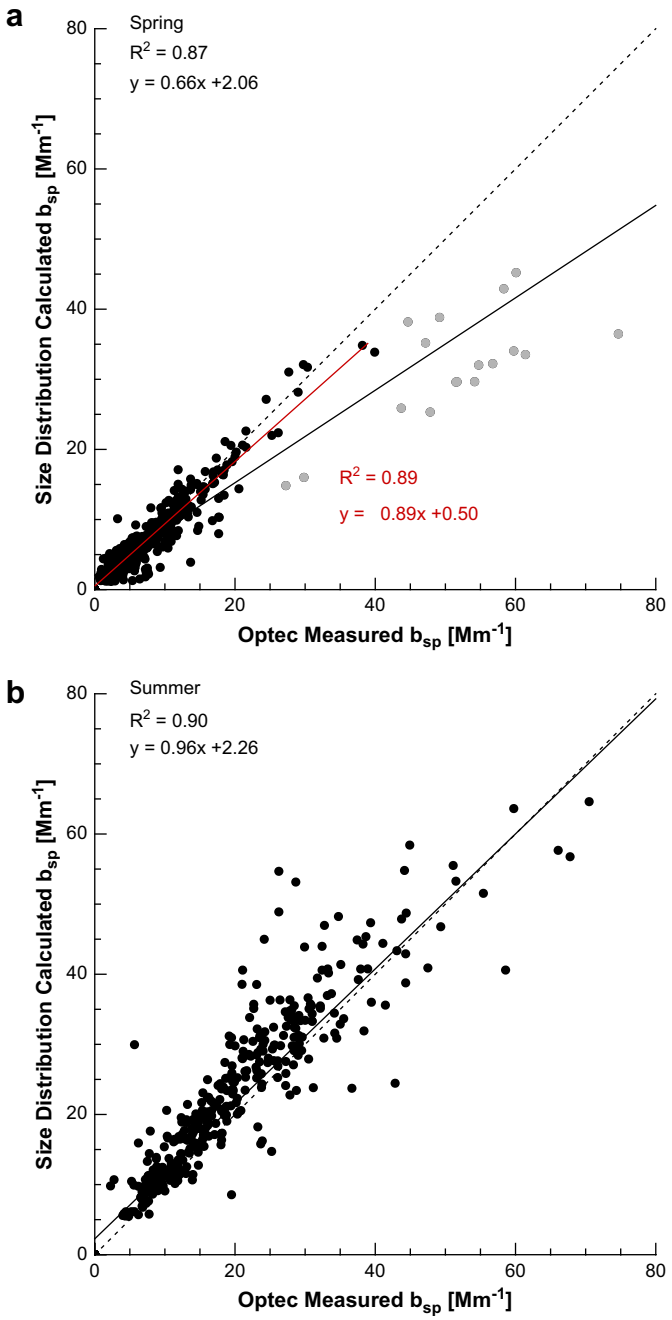

Fig. 5. Calculated versus measured b_{sp} [Mm^{-1}] using humidified accumulation and coarse mode aerosols during (a) spring (b) summer. Grey points in panel A indicate the time period April 24–25. Solid lines are regression lines, dotted line is 1:1 line. The red regression line in panel A does not include the grey points (see text). (For interpretation of the references to color in this figure legend, the reader is referred to the web version of this article.)

Mie_{wet_total} we can estimate the contribution of the coarse mode to total scattering. In both seasons scattering was dominated by accumulation mode aerosols; however, coarse mode aerosols contributed more to scattering in the spring than the summer. Averaged over each season, coarse mode aerosols accounted for 9% of the total scattering in the spring and 5% in the summer. Again, this is consistent with previous results which showed that the accumulation mode dominated the aerosol volume during the summer, but coarse mode accounted for a greater fraction of the volume in the spring.

6. Summary

Aerosol physical, chemical and optical properties were measured at a remote monitoring station in Rocky Mountain National Park during the spring and summer of 2006. Measurements included aerosol light scattering, $PM_{2.5}$ chemical composition, and aerosol particle sizing using electrical mobility, optical sizing, and time of flight techniques.

Aerosol concentrations were significantly lower during the spring study period than during the summer. The spring also exhibited much greater variation in aerosol concentration and size distribution mode statistics. Overall, aerosol concentrations were lower than those measured in other western National Parks (Hand et al., 2002; McMeeking et al., 2005). Average summer accumulation mode volume concentrations of $3 \pm 2\ \mu m\,cm^{-3}$ and $6.7 \pm 3.9\ \mu m\,cm^{-3}$ were measured using similar techniques at Big Bend and Yosemite National Parks respectively. The accumulation mode D_{gv} was also slightly smaller in RMNP compared to Big Bend, $0.26 \pm 0.04\ \mu m$, and Yosemite, $0.28 \pm 0.05\ \mu m$.

As with aerosol concentration, aerosol composition exhibited greater variability during the spring. Averaged over the entire spring study period, soil was the largest constituent of $PM_{2.5}$ mass. However, sulfates, nitrates and organics also contributed significantly to aerosol composition during the spring and at times were the dominant components. Throughout the entire summer study period, however, organics dominated $PM_{2.5}$ composition.

By plotting $PM_{2.5}$ gravimetric mass concentration versus $PM_{2.5}$ volume concentration we estimate that the seasonal average aerosol densities were $\rho = 1.96 \pm 0.19\ g\,cm^{-3}$ during the spring and $\rho = 1.40 \pm 0.06\ g\,cm^{-3}$ during the summer. The average spring value agrees with that calculated from composition data within the uncertainties. However, the low correlation between mass and volume concentrations during the spring, $R^2 = 0.66$, indicates that assuming a single density for the entire period may be a poor assumption. In the summer, agreement between estimated density and that calculated from composition can be achieved if a density of 1.2 is assumed for organics. The data are more highly correlated in the summer, $R^2 = 0.96$, reflecting the lower variability in aerosol composition during this time.

The season averaged refractive indices retrieved by the alignment method were $m_{retrieved} = 1.58 \pm 0.011$ and $m_{retrieved} = 1.56 \pm 0.011$ for spring and summer respectively. These agree with the real refractive indices calculated from composition data within the uncertainty.

During the spring, the inclusion of aerosol water uptake changed the calculated b_{sp} values by 20% on average and in some cases 50%. Including the effects of water uptake improves closure between measured and calculated b_{sp} in the spring, especially for low b_{sp} values. During the summer, the effects of including water uptake in the scattering calculations are much smaller, 6% on average, despite similar ambient RH values, indicating that the hygroscopicity of the summertime aerosol plays less of a role in total ambient light scattering.

Overall, the low aerosol concentrations and b_{sp} measured in the spring indicate that visibility degradation is not a major concern in RMNP during this time. However, on the days with the highest b_{sp} the RH was high and the $PM_{2.5}$ aerosol composition was dominated by hygroscopic species. Because of the variable nature of aerosol composition and concentration, any visibility degradation in the park during the spring is episodic and likely related to larger scale weather patterns.

In the summer, higher aerosol concentrations led to higher b_{sp} and thus a decreased visible range. The park also receives the majority of its visitors during this time, so visibility in the summer is a greater concern. Unlike in the spring, organics, not hygroscopic salts, were the primary aerosol species during the summer, and the lower hygroscopicity of the organic species led to less sensitivity of visibility degradation to ambient RH. Instead, visibility was more affected by total aerosol loading. Measured b_{sp} is highest in the summer when total aerosol loading is highest.

Disclaimer

The assumptions, findings, conclusions, judgments, and views presented herein are those of the authors and should not be interpreted as necessarily representing the National Park Service policies.

Acknowledgements

We gratefully acknowledge logistical support for the RoMANS study by Air Resource Specialists, Inc as well as Judy Visty and Laura Wheatley at RMNP. The authors also thank Taehyoung Lee, Amy Sullivan, Suresh Raja and Florian Schwandner for the URG data. Funding for this work was provided by the National Park Service through Cooperative Agreement # H2380040002 and from the State of Colorado.

References

An, W.J., Pathak, R.K., Lee, B.H., Pandis, S.N., 2007. Aerosol volatility measurement using an improved thermodenuder: application to secondary organic aerosol. Journal of Aerosol Science 38 (3), 305–314.

Carrico, C.M., Kreidenweis, S.M., Malm, W.C., Day, D.E., Lee, T., Carrillo, J., McMeeking, G.R., Collett, J.L., 2005. Hygroscopic growth behavior of a carbon-dominated aerosol in Yosemite National Park. Atmospheric Environment 39 (8), 1393–1404.

DeBell, L.J., Gebhart, K.A., Hand, J.L., Malm, W.C., Pitchford, M.L., Schichtel, B.A., White, W.H., 2006. Spatial and Seasonal Patterns and Temporal Variability of Haze and its Constituents in the United States. Report IV. Cooperative Institute for Research in the Atmosphere, Fort Collins, CO. http://vista.cira.colostate.edu/IMPROVE/Publications/Reports/2006/PDF/IMPROVE_Report_IV.pdf.

Dick, W.D., Saxena, P., McMurry, P.H., 2000. Estimation of water uptake by organic compounds in submicron aerosols measured during the Southeastern Aerosol and Visibility Study. Journal of Geophysical Research – Atmospheres 105 (D1), 1471–1479.

Hand, J.L., 2001. A New Technique for Obtaining Aerosol Size Distributions with Applications to Estimates of Aerosol Properties. Ph.D. dissertation, Colorado State University, Fort Collins, CO.

Hand, J.L., Kreidenweis, S.M., 2002. A new method for retrieving particle refractive index and effective density from aerosol size distribution data. Aerosol Science and Technology 36 (10), 1012–1026.

Hand, J.L., Kreidenweis, S.M., Sherman, D.E., Collett, J.L., Hering, S.V., Day, D.E., Malm, W.C., 2002. Aerosol size distributions and visibility estimates during the Big Bend regional aerosol and visibility observational (BRAVO) study. Atmospheric Environment 36 (32), 5043–5055.

Hasan, H., Dzubay, T.G., 1983. Apportioning light extinction coefficients to chemical-species in atmospheric aerosol. Atmospheric Environment 17 (8), 1573–1581.

Hinds, W.C., 1999. Aerosol Technology: Properties, Behavior, and Measurement of Airborne Particles. Wiley, New York.

Lee, T., Kreidenweis, S.M., Collett, J.L., 2004. Aerosol ion characteristics during the Big Bend Regional Aerosol and Visibility Observational study. Journal of the Air & Waste Management Association 54 (5), 585–592.

Lide, D.R., 2008. CRC Handbook of Chemistry and Physics [A Ready-reference Book of Chemical and Physical Data]. CRC Taylor & Francis.

Malm, W.C., Day, D.E., 2001. Estimates of aerosol species scattering characteristics as a function of relative humidity. Atmospheric Environment 35 (16), 2845–2860.

Malm, W.C., Hand, J.L., 2007. An examination of the physical and optical properties of aerosols collected in the IMPROVE program. Atmospheric Environment 41 (16), 3407–3427.

Malm, W.C., McMeeking, G.R., Kreidenweis, S.M., Levin, E.J.T., Carrico, C.M., Day, D.E., Collett, J.L., Lee, T., Sullivan, A.P., Raja, S. Using high time resolution aerosol and number size distribution measurements to estimate atmospheric extinction. Journal of the Air & Waste Management Association, submitted for publication.

Malm, W.C., Schichtel, B.A., Pitchford, M.L., Ashbaugh, L.L., Eldred, R.A., 2004. Spatial and monthly trends in speciated fine particle concentration in the United States. Journal of Geophysical Research – Atmospheres 109 (D3).

McMeeking, G.R., Kreidenweis, S.M., Carrico, C.M., Lee, T., Collett, J.L., Malm, W.C., 2005. Observations of smoke-influenced aerosol during the Yosemite Aerosol

Characterization Study: size distributions and chemical composition. Journal of Geophysical Research – Atmospheres 110 (D9).
Park, R.J., Jacob, D.J., Logan, J.A., 2007. Fire and biofuel contributions to annual mean aerosol mass concentrations in the United States. Atmospheric Environment 41 (35), 7389–7400.
Pitchford, M., Malm, W., Schichtel, B., Kumar, N., Lowenthal, D., Hand, J., 2007. Revised algorithm for estimating light extinction from IMPROVE particle speciation data. Journal of the Air & Waste Management Association 57 (11), 1326–1336.
Richardson, M.S., DeMott, P.J., Kreidenweis, S.M., Cziczo, D.J., Dunlea, E.J., Jimenez, J.L., Thomson, D.S., Ashbaugh, L.L., Borys, R.D., Westphal, D.L., Casuccio, G.S., Lersch, T.L., 2007. Measurements of heterogeneous ice nuclei in the western United States in springtime and their relation to aerosol characteristics. Journal of Geophysical Research – Atmospheres 112 (D2).
Seinfeld, J.H., Pandis, S.N., 2006. Atmospheric Chemistry and Physics: From Air Pollution to Climate Change. Wiley, Hoboken, NJ.
Snider, J.R., Petters, M.D., 2008. Optical particle counter measurement of marine aerosol hygroscopic growth. Atmospheric Chemistry and Physics 8 (7), 1949–1962.
Stelson, A.W., 1990. Urban aerosol refractive-index prediction by partial molar refraction approach. Environmental Science and Technology 24 (11), 1676–1679.
Stokes, R.H., Robinson, R.A., 1966. Interactions in aqueous nonelectrolyte solutions. I. solute–solvent equilibria. Journal of Physical Chemistry 70 (7), 2126–2131.
Tang, I.N., 1996. Chemical and size effects of hygroscopic aerosols on light scattering coefficients. Journal of Geophysical Research Atmospheres 101 (D14), 19245–19250.
Turpin, B.J., Lim, H.J., 2001. Species contributions to $PM_{2.5}$ mass concentrations: revisiting common assumptions for estimating organic mass. Aerosol Science and Technology 35 (1), 602–610.
Wexler, A.S., Clegg, S.L., 2002. Atmospheric aerosol models for systems including the ions H^+, NH_4^+, Na^+, SO_4^{2-}, NO_3^-, Cl^-, Br^-, and H_2O. Journal of Geophysical Research – Atmospheres 107 (D14).
Winklmayr, W., Wang, H.C., John, W., 1990. Adaptation of the Twomey algorithm to the inversion of cascade impactor data. Aerosol Science and Technology 13 (3), 322–331.
Yu, X.Y., Taehyoung, L., Ayres, B., Kreidenweis, S.M., Collett, J.L., Maim, W., 2005. Particulate nitrate measurement using nylon filters. Journal of the Air & Waste Management Association 55 (8), 1100–1110.